Applied Catalysis A: General 521 (2016) 34–41

Contents lists available at ScienceDirect

Applied Catalysis A: General

journal homepage: www.elsevier.com/locate/apcata

Controlled growth of CuO/Cu_2O hollow microsphere composites as efficient visible-light-active photocatalysts

Xiaolu Liu[a,c], Jiangyao Chen[a], Porun Liu[b], Haimin Zhang[d], Guiying Li[a], Taicheng An[a,*], Huijun Zhao[b,d,**]

[a] State Key Laboratory of Organic Geochemistry and Guangdong Key Laboratory of Environmental Protection and Resources Utilization, Guangzhou Institute of Geochemistry, Chinese Academy of Sciences, Guangzhou 510640, China
[b] Centre for Clean Environment and Energy, Griffith University, Gold Coast Campus, QLD 4222, Australia
[c] University of Chinese Academy of Sciences, Beijing 100049, China
[d] Key Laboratory of Materials Physics, Centre for Environmental and Energy Nanomaterials, Anhui Key Laboratory of Nanomaterials and Nanotechnology, Institute of Solid State Physics, Chinese Academy of Sciences, Hefei 230031, China

ARTICLE INFO

Article history:
Received 13 August 2015
Received in revised form 2 October 2015
Accepted 5 October 2015
Available online 14 October 2015

Keywords:
Copper oxide composite
Hollow structure
Visible light
Photocatalysis
Dye pollutant

ABSTRACT

Copper oxide composites with tunable composition and morphology were hydrothermally synthesized and used as highly efficient photocatalysts towards the degradation of dye pollutants under visible light irradiation. Effects of key synthesis reaction parameters, i.e., soft template (P123), pH of precursor solution, hydrothermal reaction temperature, the durations on the resultant copper oxide structures have been systematically investigated and a tentative mechanism was proposed for the formation of the copper oxide composites with different synthesis reaction parameters. Furthermore, the photocatalytic activities of resultant copper oxide materials towards the degradation of dye (methyl orange) demonstrated strong dependence on the compositional and morphological properties of the photocatalysts. CuO/Cu_2O hollow microsphere composites exhibited the highest visible light photocatalytic activity that can be attributed to their unique hollow structure and CuO/Cu_2O heterostructure. The demonstrated controlled growth of metal oxide composite hollow structure provides enlightenments in fabrication of highly efficient heterostructured photocatalysts for environmental remediation.

1. Introduction

With the rapid development of global industrialization, water related problems such as the fresh water shortage and water pollution have become one of the most vital factors that constraint the sustainable development of human society and economy [1,2]. Industries such as dyeing process not only consume a great deal of water, but also generate large amount of dye wastewater [3]. Unfortunately, despite of their general use, conventional water purification methods (e.g., activated sludge process, physical adsorption and membrane separation, etc.) have obvious drawbacks, such as long period, high cost for second pollution, low mineralization ability and even generation of abundant byproduct [4]. Therefore, green and efficient technologies are highly desirable to resolve the current water shortage and pollution problems.

Heterogeneous photocatalysis as a green technology has demonstrated potentials for the utilization of abundant and clean energy source (natural solar light) for the purpose of water purification and recycling [5–7]. However, the most reported semiconductor photocatalysts to date are active only under UV light illumination, greatly limited their practical applications. Extensive efforts have therefore been devoted to develop visible light active photocatalysts. Inexpensive and abundantly available copper oxide semiconductors with narrow bandgaps (1.2 eV for CuO and 2.0 eV for Cu_2O) have received much attention in recent years in the field of environmental remediation and renewable energy production [8–11], becoming promising candidates to replace traditional UV-light-active photocatalysts. Recent studies indicate that the photocatalytic activities of photocatalysts are highly dependent on their composition and structure [12,13]. To date, copper oxide materials with various hollow structures have been prepared [14,15], show higher surface area and porosity, lower bulk density, greater light-harvesting capacity, and thus higher photocatalytic activity toward the oxidation of pollutants than their solid counterparts [13,16,17]. For example, Yu et al. reported

* Corresponding author. Tel.:+ +86 20 85291501; fax: +86 20 85290706.
** Corresponding author. Tel.:+ +61 7 55528261; fax: +61 7 55528067
E-mail addresses: antc99@gig.ac.cn (T. An), h.zhao@griffith.edu.au (H. Zhao).

http://dx.doi.org/10.1016/j.apcata.2015.10.005
0926-860X/

that the Cu_2O spheres with hollow structure possessed higher photocatalytic efficiency towards methyl orange degradation than that with solid octahedral structures, due to the hollow sphere structures with higher surface area and greater light-harvesting capacity [18]. Moreover, in contrast to single component metal oxide, bi-component metal oxides integrated two types of functional materials show higher photocatalytic efficiency by increasing the charge separation and extending the energy range of photoexcitation [19]. Wang et al. [20] reported the preparation of uniform CuO/Cu_2O composite hollow microspheres through a simple hydrothermal method. The resultant materials also exhibited higher photocatalytic activity for the degradation of dye pollutant under UV light illumination than sole CuO sample. Meanwhile, Yu et al. [21] also synthesized the CuO, Cu_2O, and CuO/Cu_2O composite hollow spheres. However, none of them showed photocatalytic activity under visible light irradiation. Indeed, it is still a great challenge to synthesize copper oxide composite with good tunable structure and high visible light photocatalytic activity. Furthermore, by regulating the structure properties of copper oxide composite (e.g., composition and morphology), it is expected that the resultant materials may possess controllable visible-light-driven photocatalytic activity. However, the research on such topic is still limited attempted.

Herein, copper oxide composite with tunable composition and morphology was obtained by a facile hydrothermal method. Experimental parameters such as the amount of template (Pluronic P123), pH value of precursor solution, hydrothermal reaction temperature and hydrothermal time were studied in detail to investigate their effects on the composition and morphology of the resultant samples as well as their photocatalytic activity. Moreover, the possible formation mechanism of the copper oxide composite was tentatively proposed based on the experimental results. Finally, the photocatalytic activities of the prepared samples were evaluated by the degradation of a typical dye pollutant, i.e., methyl orange, under visible light illumination, and the performance enhancement mechanism of the copper oxide composite photocatalyst was also illustrated.

2. Experimental

2.1. Reagents

$Cu(CH_3COO)_2{\cdot}H_2O$, D-sorbitol, ethanol, acetic acid and NaOH were all purchased from Sinopharm Chemical Reagent Co., Ltd. Pluronic P123 (Ma = 5800) was obtained from Sigma–Aldrich. All reagents were analytic grade, and all aqueous solutions were prepared with deionized water.

2.2. Synthesis

In a typical synthesis procedure, appropriate amounts of $Cu(CH_3COO)_2{\cdot}H_2O$ and D-sorbitol (molar ratio of 10–1) were added into a 5.0 g L^{-1} Pluronic P123 aqueous solution under vigorous stirring. The pH value of the precursor solution was 4.5. Then, the resulted solution was hydrothermally treated at 150 °C for 24 h. After that, the precipitate was collected and washed adequately with distilled water for three times. Controllable parameters were investigated including different pH value of the precursor solution (3.5–6.5), hydrothermal reaction temperature (125–200 °C) and hydrothermal reaction time (0–72 h). Microwave-assisted extraction in ethanol (30 mL g^{-1}) for 15 min was subsequently used to remove P123 from the as-prepared samples. The samples were finally air-dried overnight at 55 °C prior to characterization and photocatalytic experiment.

2.3. Characterization

The crystallographic structure information of the samples was collected by powder X-ray diffraction (XRD, Rigaku D/MAX-2200 VPC). Surface analysis for the samples was performed using X-ray photoelectron spectroscopy (XPS, Thermo ESCALAB 250). The morphology and microstructure of the products were characterized by field emission scanning electron microscopy (SEM, JOEL JSM-890) and transmission electron microscopy (TEM, Philips F20).

2.4. Evaluation of photocatalytic activity

Visible light photocatalytic experiments were performed by photocatalytic degradation of methyl orange (MO) aqueous solutions with an initial concentration of 20 mg L^{-1}. The photocatalytic reactor consisted of a 160 mL Pyrex glass bottle with a jacket outside, a magnetic stirrer underneath and a halogen lamp (Philips, 100 W) in parallel to the glass bottle with an distance of 8.0 cm (the illuminance of *ca.* 9000 lx). The light spectrum of halogen lamp was measured in the range between 400 and 600 nm. During the experiment, the reaction temperature was kept at 25 ± 2 °C by a continuous circulation of water in the jacket around the reactor. Reaction suspensions were prepared by adding 0.225 g of the synthesized photocatalyst into 150 mL of MO aqueous solution under continuously stirring. Prior to irradiation, all the reaction suspensions were kept on stirring in dark for 60 min to establish an adsorption–desorption equilibrium. A 3.0 mL of reaction solution was taken out at given time intervals and filtered through a 0.2 μm millipore filter for the analysis. The concentration of MO was analyzed by a Thermo Spectronic Helios α UV–vis spectrometer (λ = 463 nm).

The photocatalytic degradation efficiency was calculated according to Eq. (1).

$$\text{Degradationefficiency}\,(\%) = \frac{C}{C_0} \times 100\% \quad (1)$$

where C presented the concentration of residual MO after reaction and C_0 was original concentration of MO.

3. Results and discussion

3.1. Characterization

Fig. 1A shows the XRD patterns of the samples prepared with and without the addition of template P123. Obviously, all the diffraction peaks can be assigned to Cu_2O (JCPDS card no. 78-2076) and CuO (JCPDS card no. 80-1917), suggesting the coexistence of both Cu_2O and CuO phases in the samples. Further SEM result reveals no hollow structure is formed without P123 (Fig. 1B). On the contrary, adding a suitable amount of P123 (5.0 g L^{-1}) in the preparation process results in the formation of high-purity hollow microspheres with an average diameter of *ca.* 2.0 μm and a shell thickness of *ca.* 200 nm (Fig. 1C–E). This implies that P123 template only acts as a structure-directing agent to facilitate the formation of hollow structure. Similar results have also been reported for the synthesis of other metal oxide hollow spheres [22,23]. Moreover, alternation of the amount of P123 cannot result in the change of the composition and morphology (Data not shown), again confirming the only role as template of P123 in this study. High resolution TEM image of the sample further reveals that the interlayer spacings of the selected area are calculated to be 0.245 and 0.253 nm, which are assigned to the (1 1 1) and (0 0 2) lattice planes of Cu_2O and CuO, respectively (Fig. 1F). Clearly, copper oxide composite with controllable morphology can be synthesized by a facile soft-template hydrothermal method.

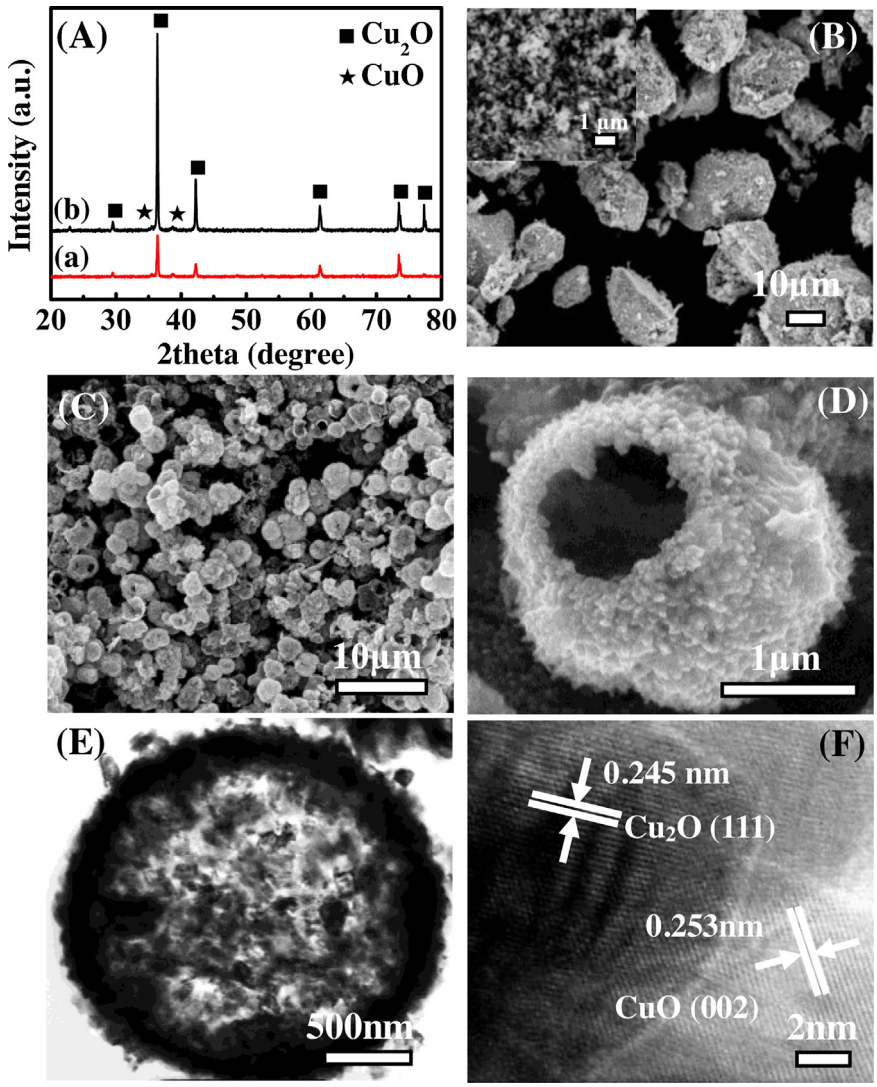

Fig. 1. (A) XRD patterns of samples prepared without (a) and with (b) P123. SEM images of samples prepared without (B) and with (C and D) P123. (E and F) TEM images of sample prepared with P123. (hydrothermal temperature: 150 °C; pH value of precursor solution: 4.5; hydrothermal time: 24 h).

To understand the formation process of the copper oxide composite, the effects of reaction conditions on the resultant samples are investigated. In the process of hydrothermal synthesis, the pH value of the precursor solution can affect the solubility of solute, the crystal growth rate, and ultimately the microstructure, shape and size of the crystals [24,25]. Thus, the effect of the pH value of the precursor solution on the microstructures of the resulted samples is firstly investigated. Herewith, acetic acid or NaOH solution is used to adjust the pH value of the precursor solution. As seen from the XRD patterns (Fig. 2A), the resulted products are all pure Cu_2O when the pH values are selected as 3.5, 5.5 and 6.5, while a mixture of Cu_2O and CuO is obtained when the pH value equals to 4.5, indicating too low or too high pH value of the precursor solution is unfavorable for the formation of CuO/Cu_2O composite. This indicates that the pH value of precursor solution may significantly influence the followed oxidation and reduction reactions of copper ions [26]. Further XPS analysis also confirms the XRD results. As shown in Fig. S1A, the presence of only copper and oxygen in all samples can be observed, except for a small amount of adsorbed carbon whose C 1s peak position (284.6 eV) is used to calibrate the acquired spectra. However, high-resolution XPS results show significantly different. In the case of Cu 2p spectrum for the sample prepared under the condition of pH 4.5 (Fig. 3A), four peaks corresponding to the Cu $2p_{3/2}$ (933.5 and 935.3 eV) and Cu $2p_{1/2}$ (953.5 and 955.4 eV) are observed. According to the literature [27], the peaks at 933.5 and 953.5 eV are the characteristic peaks of Cu_2O, while that at 935.3 and 955.4 eV are attributed to the CuO, suggesting the formation of Cu_2O and CuO composite. However, only peaks at 933.5 and 953.5 eV can be observed from Cu 2p spectrum of the sample prepared at other pH values (taking the sample prepared with pH 6.5 as an example), indicating the formation of pure Cu_2O. In addition to the composition, pH value of the precursor solution also shows great effect on the morphology of the resulted samples. As shown in Fig. 4, the synthesized sample (pH 3.5) is mixture of bumpy micropolyhedrons and particles. After increasing pH value to 4.5, uniform microspheres with hollow structure are obtained, which then become solid when the pH increases to 5.5. And irregular-shaped microparticles appear when the pH value reaches 6.5. Obviously, by simply adjusting the pH value of the precursor solution, Cu_2O or CuO/Cu_2O composite with the morphologies of polyhedrons, solid (or hollow) microspheres or microparticles can be obtained. As one may know, CuO/Cu_2O composite has demonstrated higher photocatalytic activity than pure Cu_2O [21]. Similarly, the fabricated CuO/Cu_2O composite hollow microspheres are expected to have superior photocatalytic

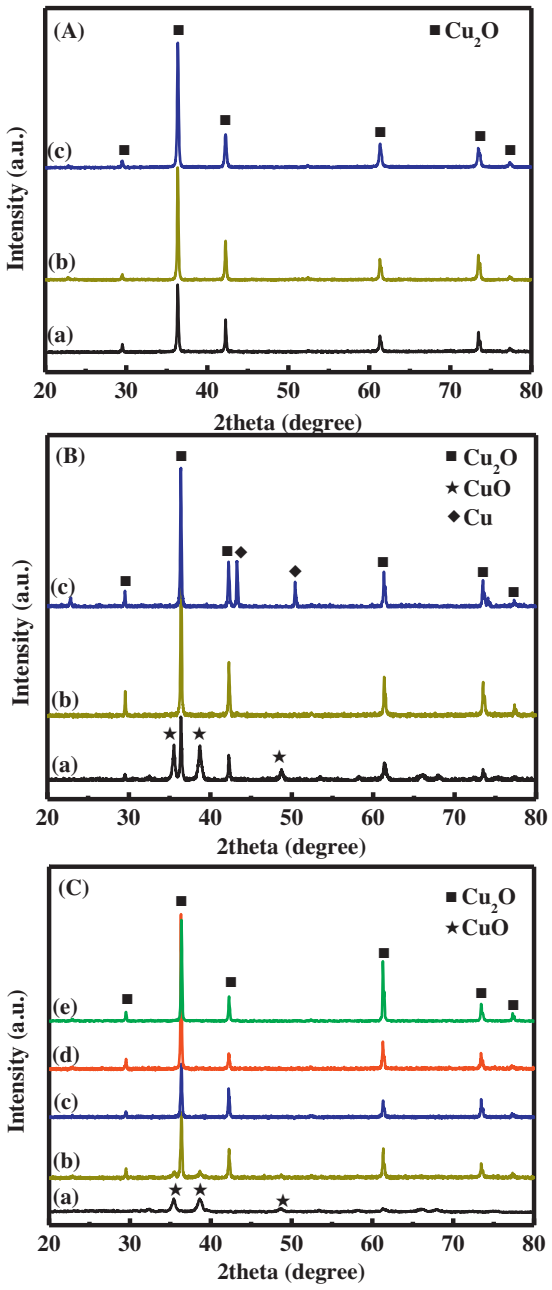

Fig. 2. XRD patterns of samples prepared at different pH value of precursor solution (A) ((a) 3.5; (b) 5.5; (c) 6.5)); hydrothermal reaction temperature (B) ((a) 125 °C; (b) 175 °C; (c) 200 °C)) and hydrothermal reaction time (C) ((a) Non-hydrothermal; (b) 12 h; (c) 36 h; (d) 48 h; (e) 72 h)).

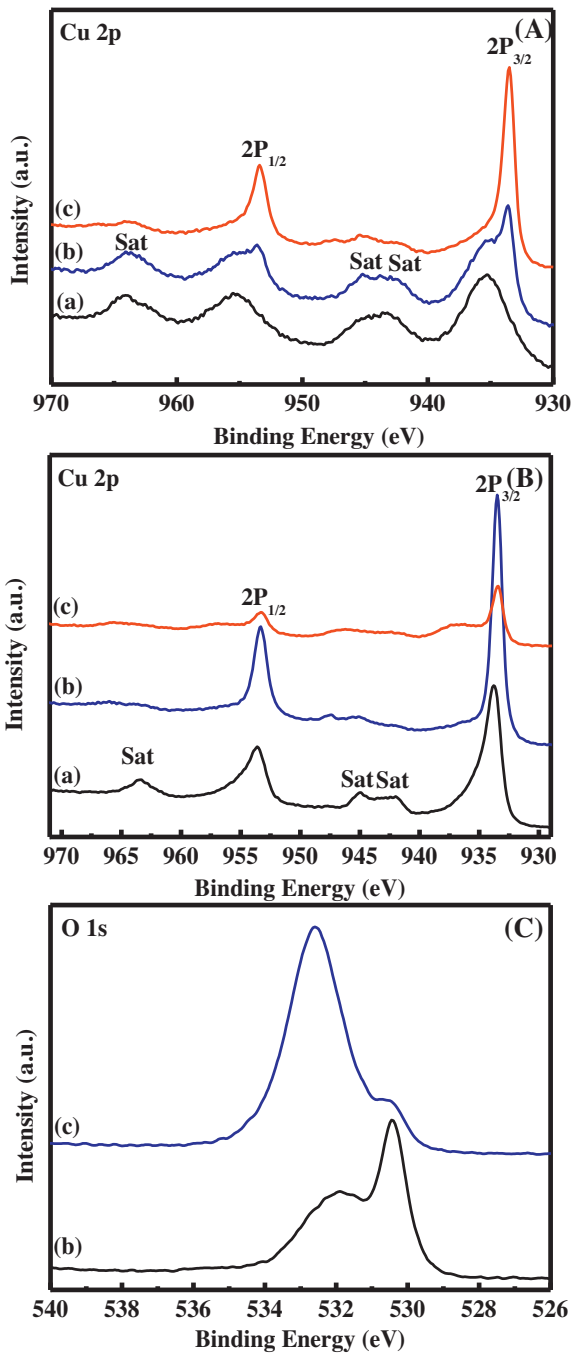

Fig. 3. XPS spectra of samples prepared at different pH value of precursor solution (A) ((b) pH 4.5; (c) pH 6.5)), hydrothermal reaction time (A) ((a) Non-hydrothermal; (b) 24 h) and hydrothermal temperature (B and C) ((a) 125 °C; (b) 175 °C; (c) 200 °C).

activity as compared with corresponding Cu_2O particles or solid microspheres in this study.

As reported in previous work, hydrothermal reaction temperature was found to be a key parameter to influence the photocatalytic activity of the resultant photocatalyst [6,28]. Thus the effect of the hydrothermal reaction temperature on the photocatalytic performance of the synthesized sample is investigated. XRD results displayed in Fig. 2B reveal that both CuO and Cu_2O phases exist in the sample obtained under the hydrothermal reaction temperature of 125 °C, while the content of CuO then decreases significantly, leading to the dominant Cu_2O in the sample (150 °C). As further increasing the temperature to 175 °C, CuO completely disappears and only pure Cu_2O exists in the sample. Notably, a mixture of Cu_2O and Cu is observed for the sample synthesized under a higher temperature (200 °C). All these results indicate that the composition of resultant sample can be readily tuned by increasing hydrothermal reaction temperature, resulting in an in-situ reduction process of CuO to Cu_2O and then Cu. Similar results have also been found by Li et al. [29] and Ai et al. [30]. XPS technique is further employed to verify this conclusion (Figs. S1B and 3). The Cu 2p spectra for the samples synthesized at the temperature of 125 and 150 °C illustrate that the existence of both CuO (935.3 and 955.4 eV) and Cu_2O (933.5 and 953.5 eV). With further increasing reaction temperature to 175 °C, the peaks observed in the Cu 2p core level spectrum are in good agreement with that of Cu_2O. However, these peaks become evidently weaker when the hydrothermal temperature increases to

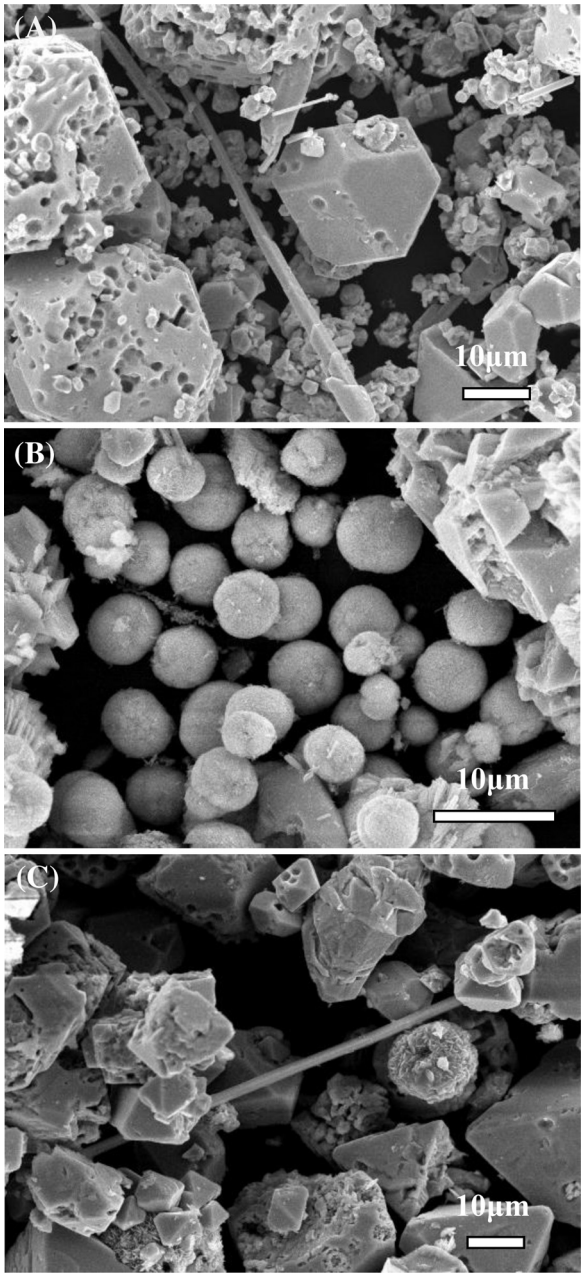

Fig. 4. SEM images of samples prepared at different pH value of precursor solution. ((A) pH 3.5; (B) pH 5.5; (C) pH 6.5).

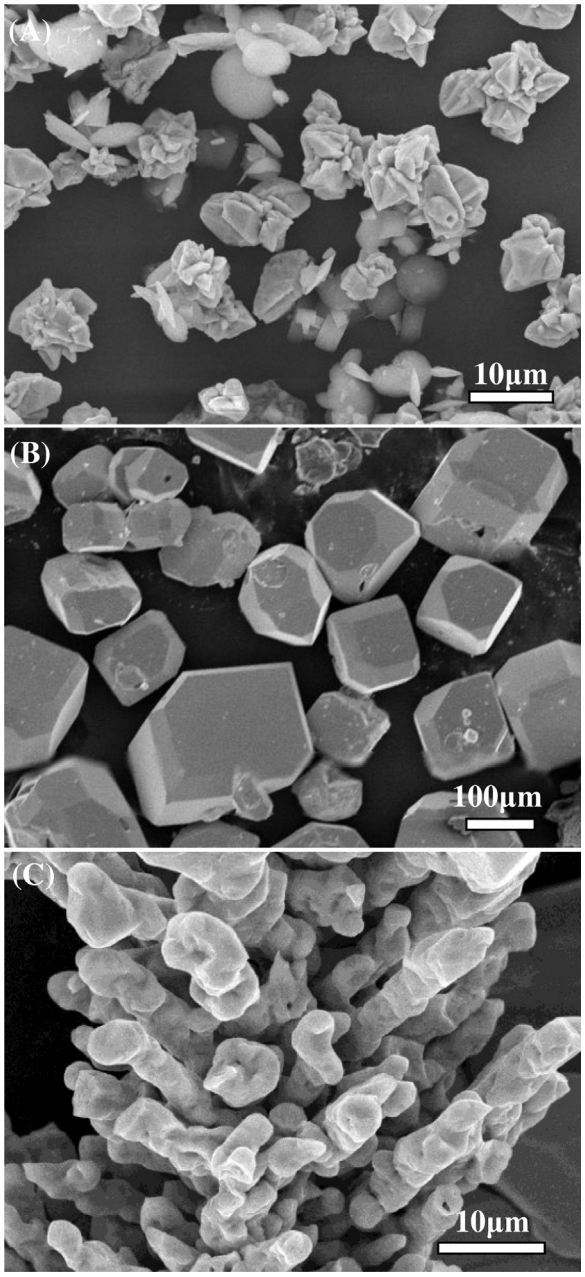

Fig. 5. SEM images of the samples prepared at different hydrothermal temperature. ((a) 125 °C; (b) 175 °C; (c) 200 °C).

200 °C, indicating the decrease of the content of Cu_2O in the sample. The O 1s spectra (Fig. 3C) reveal that the binding energy peak at 530.0 eV (O^{2-} in the compounds) decreases significantly when the reaction temperature increases from 175 to 200 °C with an obvious increase of the peak at 532.0 eV (O from absorbed gaseous molecules). This result suggests that copper ion in the oxide may be reduced to metallic Cu at high hydrothermal reaction temperature [31,32]. Similarly, the morphologies of the samples prepared at different hydrothermal temperatures are also investigated (Fig. 5). The sample prepared at 125 °C is consisted of flower-like clusters with the average size of about 10.0 μm (Fig. 5A). Further observation reveals the coexistence of few solid hemispheres. For the sample synthesized at 150 °C, high-quality hollow microspheres with a diameter of *ca.* 2.0 μm can be observed (Fig. 1C). Further increasing the reaction temperature to 175 and 200 °C, polyhedral and dendriform structures are obtained, respectively (Fig. 5B and C). Based on the above results, it is found that increasing the reaction temperature in the range investigated (125–200 °C) will lead to the transformation of mixed CuO and Cu_2O (flower-like cluster or hollow sphere), into pure Cu_2O (polyhedron) and then to mixed Cu_2O and Cu (dendriform particle). These obtained copper-based materials with different composition and morphology may possess significantly different photocatalytic activities.

The characterization results for the samples prepared with or without hydrothermal treatment are shown in Figs. 2C, 3A and 6. For the sample "Non-hydrothermal", the precursor solution with same composition is stirred for 24 h under room temperature. XRD result reveals that only weak diffraction peaks for CuO can be observed for the sample obtained by "Non-hydrothermal" treatment, suggesting the formation of CuO with poor crystallinity. This may be due to incomplete reaction of most substances in the precursor solution, which can be further confirmed by the XPS result.

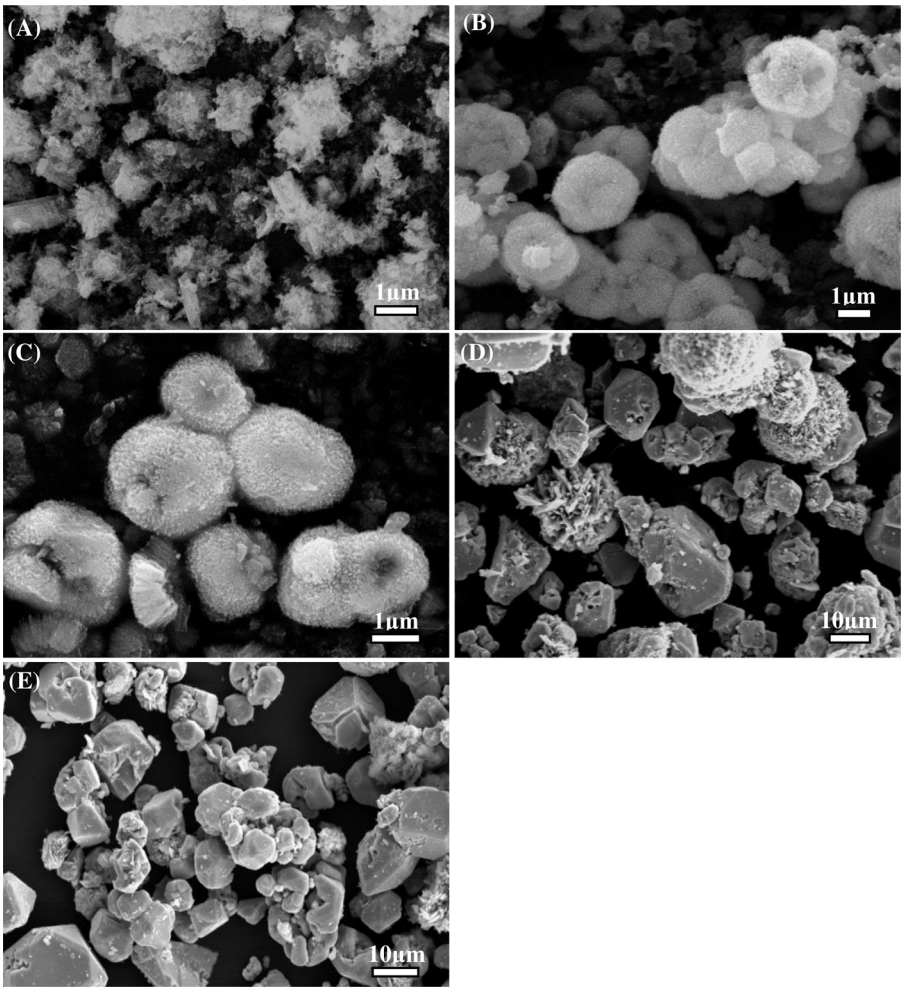

Fig. 6. SEM images of the samples prepared at different hydrothermal time. ((A) Non-hydrothermal; (B) 12 h; (C) 36 h; (D) 48 h; (E) 72 h).

Clearly, binding energies for Cu $2p_{3/2}$ and Cu $2p_{1/2}$ centered at 935.3 and 955.4 eV are observed, indicating the existence of CuO. Moreover, the Cu 2p core level spectrum displays satellite peaks, further confirming the existence of CuO in the sample [27,31–33]. However, significant increase of the intensity of the diffraction peaks of all the samples is observed after hydrothermal treatment, indicating enhanced crystallinity (Fig. 2C). Notably, variable composition of the resulted materials is obtained. In the case of the sample synthesized after the reaction of 12 h, both diffraction peaks of Cu_2O and CuO can be detected by the XRD technique. And the intensity of the peaks of the former becomes stronger and that of the latter is weaker with prolonging the reaction time to 24 h, implying that the formed CuO may be reduced to Cu_2O with the presence of D-sorbitol. And given enough reaction time (≥36 h), the formation of pure Cu_2O is observed, further confirming the above hypothesis. Furthermore, the morphology transformation of the samples is also investigated. For sample "Non-hydrothermal" treatment, only fluffy particles can be observed (Fig. 6A), most of which are then transformed into hollow microspheres after hydrothermal reaction of 12 h (Fig. 6B). With increasing the reaction time to 24 h, high-purity hollow microspheres are obtained (Fig. 1C). However, when the reaction time is further prolonged (≥36 h), the hollow microspheres are severely damaged (Fig. 6C), and irregularly shaped particles with large sizes are formed (Fig. 6D and E). Therefore, a suitable hydrothermal reaction time (≤24 h) is also very critical to the formation of CuO/Cu_2O composite hollow microspheres with good crystallinity.

Based on the above results, a possible soft-templating and oriented attachment formation mechanism of the copper oxide composite (taking CuO/Cu_2O composite hollow microspheres as an example) is proposed and shown in Fig. 7. As known, P123 possesses a long poly(propylene oxide) segment and two medium length poly(-ethylene oxide) blocks, favorable for the formation of micelles with dehydrated poly(propylene oxide) blocks in the core and coronas of hydrated poly(ethylene oxide) segments at the micellar surface [34]. Moreover, a strong complexation interaction has been observed between P123 and metal ions, leading to the formation of P123-metal ion micelles in the solution [35,36] to avoid the formation of $Cu(OH)_2$ precipitation. Thus, in this study, Cu^{2+} in the solution will firstly interact with P123 to form P123-Cu^{2+} core-shell micelles, which are easily oxidized by O_2 to produce P123-CuO composite micelles under high temperature and pressure conditions. Further, CuO in the composite is reduced to Cu_2O at the presence of reductant—D-sorbitol, leading to the formation of P123-CuO/Cu_2O composite micelles. Subsequently, these composite micelles grow and aggregate through oriented attachment process, leading to the formation of P123-CuO/Cu_2O composite microspheres. Finally, after the removal of the P123 template by microwave-assisted extraction, CuO/Cu_2O composite hollow microspheres can be obtained successfully. This formation mechanism is also suitable for the rest copper oxide samples with tunable composition and morphology in this study, except different synthesis conditions such as pH value of precursor solution, hydrothermal temperature and time are applied.

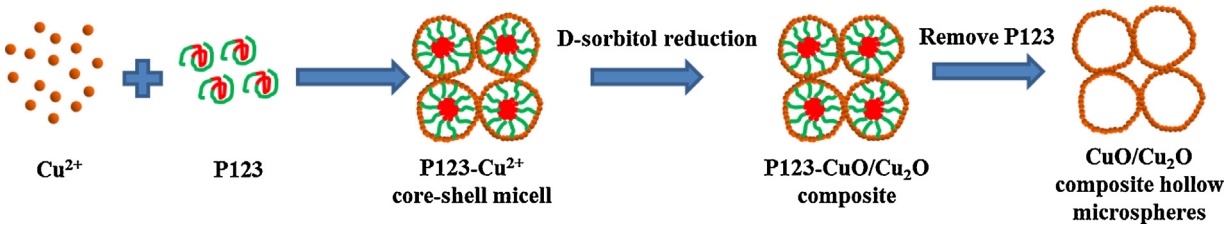

Fig. 7. Schematic illustration of the possible formation mechanism of CuO/Cu_2O composite hollow microspheres.

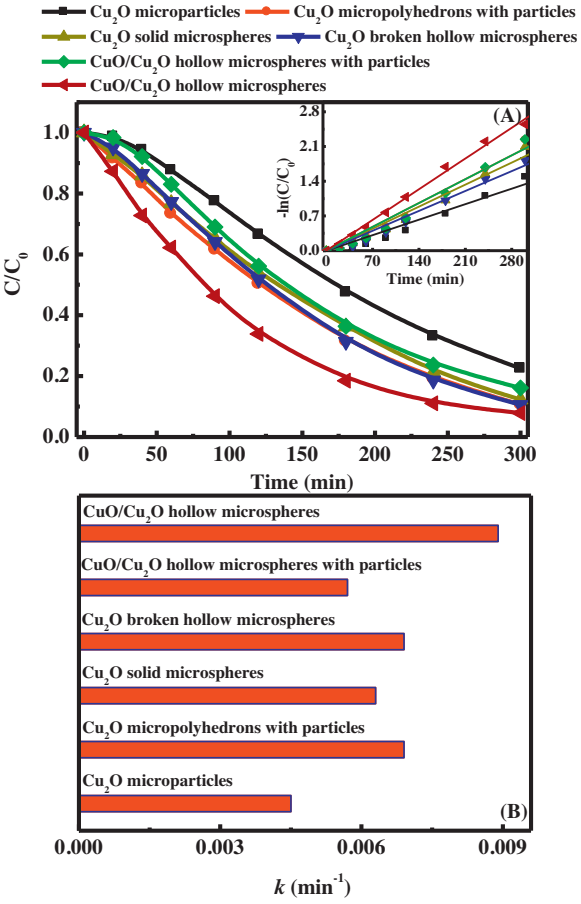

Fig. 8. Kinetic curves (A) and rate constants (B) of photocatalytic MO degradation by the copper oxide composite photocatalysts.

3.2. Evaluation of photocatalytic activity

The photocatalytic activities of the prepared copper oxide samples are evaluated by photocatalytic degradation of MO in water, and the results are presented in Fig. 8. From Fig. 8A, it can be seen that all samples show high photocatalytic activities, and the degradation efficiency of MO by the Cu_2O microparticles reaches 77.5% after 300 min of visible light irradiation, which then increases to 83.9% by CuO/Cu_2O hollow microspheres with particles and 87.7% by Cu_2O solid microspheres. Cu_2O micropolyhedrons with particles (89.3%) and Cu_2O broken hollow microspheres (89.4%) show similar degradation efficiency toward MO, while the highest photocatalytic activity for the degradation of MO is obtained for the CuO/Cu_2O hollow microspheres (92.2%). The inset of Fig. 8A presents the linear fittings of the relationship between $-\ln(C/C_0)$ and the degradation time, and the rate constants are given in Fig. 8B. Clearly, pseudo-first-order degradation kinetics is observed, which is similar to the kinetics obtained from other metal oxide catalysis systems [37]. Moreover, the trend for the rate constant reveals that the rate constant for CuO/Cu_2O hollow microspheres ($0.0089\ min^{-1}$) is more than 1.3 times of the other samples, again confirming the best visible-light-driven photocatalytic activity of the CuO/Cu_2O hollow microspheres.

The superiorly visible-light-active photocatalytic activity of CuO/Cu_2O composite hollow microspheres in comparison with other copper oxide composite photocatalysts can be attributed to its excellent light harvesting capability, enhanced specific surface area of the unique hollow structure and improved photogenerated charge carrier separation within the CuO/Cu_2O heterostructure. As shown in Fig. 1, the sample shows unique hollow structure, which can act as a reservoir not only to enhance the light harvesting, but also to facilitate the transfer and diffusion of dye molecules in the microsphere [16,38]. Moreover, due to the existence of both Cu_2O and CuO in the sample, the interface between these two copper oxides can facilitate the separation of the photogenerated electrons and holes due to the difference in the energy levels of their conduction bands and valence bands [20,21], leading to the high utilization of the absorbed visible light. Thus, the dye molecules concentrated inside the hollow microspheres can readily react with photogenerated active species ($^{\bullet}OH$, $O^{2-\bullet}$, h^+, etc), which accelerates the photocatalytic degradation of dye pollutant and results in high degradation efficiency. This high visible photocatalytic activity of the prepared CuO/Cu_2O composite hollow microsphere photocatalyst may fulfill the continuous usage for large-scale wastewater purification process.

4. Conclusions

In summary, copper oxide composite hollow microsphere with high visible light photocatalytic activity was synthesized by simple hydrothermal method. The synthesis reaction parameters showed significant effects on the composition and morphology of the resultant samples. By simply changing the synthesis reaction parameters including the amount of Pluronic P123, pH value of the precursor solution, hydrothermal temperature and time, the composition of the resultant sample was correspondingly transformed from CuO/Cu_2O composite, to Cu_2O and Cu/Cu_2O composite with tunable morphologies such as bulky particles, polyhedrons, solid and hollow microspheres, *etc.* Both the soft-templating and oriented attachment processes might play key roles in the formation of the copper oxide composite. Compared with other structures, the CuO/Cu_2O composite hollow microspheres displayed the best visible light photocatalytic activity of 92.2% within 300 min toward the degradation of MO, which may be due to their excellent light harvesting capability, enhanced specific surface area of the unique hollow structure and improved photogenerated charge carrier separation within CuO/Cu_2O heterostructure.

Acknowledgements

This is contribution No.IS-2136 from GIGCAS. The authors appreciate the financial supports from NSFC (41373102, 21307132

and U1401245), National Natural Science Funds for Distinguished Young Scholars (41425015), Team Project from Natural Science Foundation of Guangdong Province, China (S2012030006604).

Appendix A. Supplementary data

Supplementary data associated with this article can be found, in the online version, at http://dx.doi.org/10.1016/j.apcata.2015.10.005.

References

[1] R.D. Ambashta, M. Sillanpaa, J. Hazard. Mater. 180 (2010) 38–49.
[2] P. Aldhous, Nature 422 (2003), 251–251.
[3] M. Vakili, M. Rafatullah, B. Salamatinia, A.Z. Abdullah, M.H. Ibrahim, K.B. Tan, Z. Gholami, P. Amouzgar, Carbohyd. Polym. 113 (2014) 115–130.
[4] C.C. Wang, J.R. Li, X.L. Lv, Y.Q. Zhang, G.S. Guo, Energy Environ. Sci. 7 (2014) 2831–2867.
[5] J.Y. Chen, H.M. Zhang, P.R. Liu, Y.B. Li, X.L. Liu, G.Y. Li, P.K. Wong, T.C. An, H.J. Zhao, Appl. Catal. B-Environ. 168 (2015) 266–273.
[6] J.Y. Chen, H.Y. Luo, H.X. Shi, G.Y. Li, T.C. An, Appl. Catal. A-Gen. 485 (2014) 188–195.
[7] W. Zhang, L.D. Zou, L.Z. Wang, Appl. Catal. A-Gen. 371 (2009) 1–9.
[8] D.P. Li, K. Dai, J.L. Lv, L.H. Lu, C.H. Liang, G.P. Zhu, Mater. Lett. 150 (2015) 48–51.
[9] Z.C. Ma, L.M. Wang, D.Q. Chu, H.M. Sun, A.X. Wang, RSC Adv. 5 (2015) 8223–8227.
[10] Y.X. Zhao, W.T. Wang, Y.P. Li, Y. Zhang, Z.F. Yan, Z.Y. Huo, Nanoscale 6 (2014) 195–198.
[11] K. Mageshwari, R. Sathyamoorthy, J. Park, Powder Technol. 278 (2015) 150–156.
[12] J.Y. Chen, G.Y. Li, H.M. Zhang, P.R. Liu, H.J. Zhao, T.C. An, Catal. Today 224 (2014) 216–224.
[13] D. Li, Q. Qin, X.C. Duan, J.Q. Yang, W. Guo, W.J. Zheng, ACS Appl. Mater. Interfaces 5 (2013) 9095–9100.
[14] Y.M. Sui, W.Y. Fu, Y. Zeng, H.B. Yang, Y.Y. Zhang, H. Chen, Y.X. Li, M.H. Li, G.T. Zou, Angew. Chem. Int. Ed. 49 (2010) 4282–4285.
[15] C.H. Kuo, M.H. Huang, J. Am. Chem. Soc. 130 (2008) 12815–12820.
[16] J.Y. Chen, X. Nie, H.X. Shi, G.Y. Li, T.C. An, Chem. Eng. J. 228 (2013) 834–842.
[17] A. Syoufian, O.H. Satriya, K. Nakashima, Catal. Commun. 8 (2007) 755–759.
[18] Y. Yu, L.Y. Zhang, J. Wang, Z. Yang, M.C. Long, N.T. Hu, Y.F. Zhang, Nanoscale Res. Lett. 7 (2012).
[19] A. Enesca, L. Isac, A. Duta, Thin Solid Films 542 (2013) 31–37.
[20] S.L. Wang, P.G. Li, H.W. Zhu, W.H. Tang, Powder Technol. 230 (2012) 48–53.
[21] H.G. Yu, J.G. Yu, S.W. Liu, S. Mann, Chem. Mater. 19 (2007) 4327–4334.
[22] Q.Z. Zhang, X.Y. Li, Q.D. Zhao, Y. Shi, F. Zhang, B.J. Liu, J. Ke, L.Z. Wang, Appl. Surf. Sci. 337 (2015) 27–32.
[23] A. Katti, S.R. Venna, M.A. Carreon, Catal. Commun. 10 (2009) 2036–2040.
[24] H.Y. Jiang, H.X. Dai, X. Meng, K.M. Ji, L. Zhang, J.G. Deng, Appl. Catal. B-Environ. 105 (2011) 326–334.
[25] C.L. Yu, F.F. Cao, X. Li, G. Li, Y. Xie, J.C. Yu, Q. Shu, Q.Z. Fan, J.C. Chen, Chem. Eng. J. 219 (2013) 86–95.
[26] Z.Z. Chen, E.W. Shi, Y.Q. Zheng, W.J. Li, B. Xiao, J.Y. Zhuang, J. Cryst. Growth 249 (2003) 294–300.
[27] Y.C. Zhang, J.Y. Tang, G.L. Wang, M. Zhang, X.Y. Hu, J. Cryst. Growth 294 (2006) 278–282.
[28] J.Y. Chen, G.Y. Li, Y. Huang, H.M. Zhang, H.J. Zhao, T.C. An, Appl. Catal. B-Environ. 123 (2012) 69–77.
[29] Y.H. Li, M.Y. Zhao, N. Zhang, R.J. Li, J.X. Chen, J. Alloy Compd. 643 (2015) 106–110.
[30] Z.H. Ai, L.Z. Zhang, S.C. Lee, W.K. Ho, J. Phys. Chem. C 113 (2009) 20896–20902.
[31] Y.J. Xiong, Z.Q. Li, R. Zhang, Y. Xie, J. Yang, C.Z. Wu, J. Phys. Chem. B 107 (2003) 3697–3702.
[32] W.T. Yao, S.H. Yu, Y. Zhou, J. Jiang, Q.S. Wu, L. Zhang, J. Jiang, J. Phys. Chem. B 109 (2005) 14011–14016.
[33] M. Parhizkar, S. Singh, P.K. Nayak, N. Kumar, K.P. Muthe, S.K. Gupta, R.S. Srinivasa, S.S. Talwar, S.S. Major, Colloids Surf. A-Physicochem. Eng. Asp. 257–58 (2005) 277–282.
[34] S.Y. Hou, Y. Xing, X.C. Liu, Y.C. Zou, B. Liu, X.J. Sun, CrystEngComm 12 (2010) 1945–1948.
[35] Y.R. Ma, L.M. Qi, J.M. Ma, H.M. Cheng, Langmuir 19 (2003) 4040–4042.
[36] Y.R. Ma, L.M. Qi, J.M. Ma, H.M. Cheng, W. Shen, Langmuir 19 (2003) 9079–9085.
[37] J.Y. Chen, G.Y. Li, Z.G. He, T.C. An, J. Hazard. Mater. 190 (2011) 416–423.
[38] J.W. Shi, X. Zong, X. Wu, H.J. Cui, B. Xu, L.Z. Wang, M.L. Fu, CrystEngComm 4 (2012) 488–491.